

# Metabolic profile evolution in relapsed/refractory B-cell non-Hodgkin lymphoma patients treated with CD19 chimeric antigen receptor T-cell therapy and implications in clinical outcome

Serena De Matteis,<sup>1\*</sup> Laura Del Coco,<sup>2\*</sup> Federica De Castro,<sup>2</sup> Anna Maria Giudetti,<sup>2</sup> Beatrice Casadei,<sup>1</sup> Francesco Iannotta,<sup>1</sup> Francesco De Felice,<sup>1,3</sup> Enrica Tomassini,<sup>1</sup> Francesca Vaglio,<sup>1,3</sup> Maria Naddeo,<sup>1</sup> Irene Salamon,<sup>1</sup> Gianluca Storci,<sup>1</sup> Noemi Laprovitera,<sup>1</sup> Daria Messelodi,<sup>1</sup> Salvatore Nicola Bertuccio,<sup>1</sup> Marta Tassoni,<sup>3</sup> Barbara Sinigaglia,<sup>1</sup> Francesco Barbato,<sup>1,3</sup> Margherita Ursi,<sup>1,3</sup> Elena Campanini,<sup>1</sup> Enrico Maffini,<sup>1</sup> Marcello Roberto,<sup>1,3</sup> Cinzia Pellegrini,<sup>1</sup> Elisa Dan,<sup>1</sup> Chiara Pirazzini,<sup>3</sup> Paolo Garagnani,<sup>1,3</sup> Manuela Ferracin,<sup>1,3</sup> Pier Luigi Zinzani,<sup>1,3</sup> Francesco Paolo Fanizzi,<sup>2</sup> Massimiliano Bonafè<sup>1,3</sup> and Francesca Bonifazi<sup>1</sup>

<sup>1</sup>IRCCS Azienda Ospedaliero-Universitaria di Bologna, Bologna; <sup>2</sup>Department of Biological and Environmental Sciences and Technologies (Di.S.Te.B.A.), University of Salento, Lecce and <sup>3</sup>Department of Medical and Surgical Sciences (DIMEC), University of Bologna, Bologna, Italy

*\*SDM and LDC contributed equally as first authors.*

**Correspondence:** M. Bonafè  
[massimiliano.bonafe@unibo.it](mailto:massimiliano.bonafe@unibo.it)  
F.P. Fanizzi  
[fp.fanizzi@unisalento.it](mailto:fp.fanizzi@unisalento.it)

**Received:** February 27, 2024.  
**Accepted:** December 11, 2024.  
**Early view:** December 19, 2024.

<https://doi.org/10.3324/haematol.2024.285154>

©2025 Ferrata Storti Foundation  
Published under a CC BY-NC license



## Supplementary Methods

### NMR measurement and data processing

Plasma samples were thawed at room temperature and 5 mm NMR tubes were prepared for NMR measurement by adding 200  $\mu$ L of sample with 400  $\mu$ L of saline buffer solution at pH 7.4 (NaCl 0.9%, 50 mM of sodium phosphate buffer in D<sub>2</sub>O containing trimethylsilyl propionic-2,2,3,3-d<sub>4</sub> acid sodium salt, TSP). <sup>1</sup>H-NMR spectra for all plasma samples were recorded on a Bruker Avance III NMR spectrometer (Bruker, Ettlingen, Germany), at a frequency of 600.13 MHz for <sup>1</sup>H observation, equipped with a TCI cryoprobe (Triple Resonance inverse Cryoprobe), and incorporating a z-axis gradient coil and automatic tuning-matching. Experiments were carried out at 300 K in automation mode using a Bruker Automatic Sample Changer, which interfaced with the software IconNMR version 5.0.9. For each sample, a standard 1D-<sup>1</sup>H Carr-Purcell-Meiboom-Gill (1D-CPMG) experiment (with suppression of water resonance) was performed to filter out signals belonging to proteins and other macromolecules, thus obtaining spectra primarily comprising signals from metabolites and small molecules.<sup>1,2</sup> Free induction decays (with a FID size of 64 K data points) were collected by averaging 128 transients, 16 dummy scans, a 5 s relaxation delay, 12,019.230 Hz (20.0276 ppm) spectral width, an acquisition time of 1.36 s, 1.2 ms delay (d20, fixed echo time to allow elimination of J modulation effects according to the Bruker pulse program code, with a loop of 126 cycles for T2 filter), obtaining a total value of total spin-spin relaxation delay of 302.4 ms. The resulting FIDs were multiplied by an exponential weighting function corresponding to a line broadening of 0.3 Hz before Fourier transformation, automated phasing, and baseline correction. 2D NMR spectra (<sup>1</sup>H Jres, <sup>1</sup>H-<sup>1</sup>H COSY, <sup>1</sup>H-<sup>13</sup>C HSQC, and <sup>1</sup>H-<sup>13</sup>C HMBC) were also randomly acquired for assignment purposes, and metabolites identified according to the public database Human metabolome database and ChenomX NMR Suite 8 (ChenomX Inc., Edmonton, Canada) software, together with a comparison with other published data.<sup>2,3</sup>

The NMR spectra were processed using Topspin 3.6.1 and Amix 3.9.13 (Bruker, Biospin, Italy), both for simultaneous visual inspection and the successive bucketing process for multivariate statistical analyses. The entire NMR spectrum (in the range of 10.0–0.5 ppm) was segmented in fixed rectangular buckets 0.02 ppm in width and successively integrated. Chemical shifts were referenced to TSP as an internal standard ( $\delta$ H 0.00 ppm) and the spectral region between 4.90–4.50 ppm was discarded to avoid the effects of water suppression. Moreover, a total of other six spectral regions were not taken into consideration, due to the residual peaks of solvents and identification of the anticoagulant ethylenediaminetetraacetic acid (EDTA) between 4.06–4.00, 3.70–3.57, 3.30–3.00, 2.77–2.70, 2.60–2.55 and 1.20–1.15 ppm. Centering, normalization to a constant sum, and the Pareto scaling were applied to the bucketed NMR data to improve the performance of downstream statistical analyses.<sup>4</sup>

### **Plasma profile of circulating N-glycans**

Plasma samples were obtained from an independent cohort of 20 patients who were in CR/PR on the basis of the D30 PET/TC scans. Circulating plasma profile of ten N-glycans was assessed at D30 time point by using "DNA Sequencer Adapted-Fluorophore Assisted Carbohydrate Electrophoresis" (DSA-FACE), as previously described<sup>5</sup>. Briefly, 2  $\mu$ l of plasma were treated with a denaturing buffer, labeled with 8-amino-1,3,6-pyrenetrisulfonic acid (APTS), desialylated and read-out with a microcapillary electrophoresis on an automated Sanger sequencing platform to obtain the corresponding peaks profile. The relative height of each peak, which represents the relative concentration of the oligosaccharide structures, was calculated as the ratio between the height of the peak and the sum of the heights of the ten peaks (**Supplementary Fig. S4**). Finally, the GlycoAge<sup>6</sup> score has been calculated as the log ratio of peak1 (NGA2F) and peak6 (NA2F) (**Supplementary Fig. S4**).

## References

1. Vignoli A, Ghini V, Meoni G, et al. High-throughput metabolomics by 1D NMR. *Angewandte Chemie International Edition*. 2019;58(4):968-994.
2. Del Coco L, Greco M, Inguscio A, et al. Blood Metabolite Profiling of Antarctic Expedition Members: An  $^1\text{H}$  NMR Spectroscopy-Based Study. *International Journal of Molecular Sciences*. 2023;24(9):8459.
3. Foxall PJ, Spraul M, Farrant RD, Lindon LC, Neild GH, Nicholson JK. 750 MHz  $^1\text{H}$ -NMR spectroscopy of human blood plasma. *J Pharm Biomed Anal*. 1993;11(4-5):267-276.
4. van den Berg RA, Hoefsloot HC, Westerhuis JA, Smilde AK, van der Werf MJ. Centering, scaling, and transformations: improving the biological information content of metabolomics data. *BMC Genomics*. 2006;7:142.
5. Vanhooren V, Laroy W, Libert C, Chen C. N-glycan profiling in the study of human aging. *Biogerontology*. 2008;9(5):351-356.
6. Vanhooren V, Dewaele S, Libert C, et al. Serum N-glycan profile shift during human ageing. *Exp. Gerontol*. 2010; 45(10):738-743.

## Supplementary Figures

**Figure S1.** A) Flow chart of the study population. (B) Representative  $^1\text{H}$  NMR spectrum of metabolites obtained from a plasma sample. BCAA: valine, leucine, isoleucine; N-GlycA: N-acetyl groups of glycoproteins; \*: EDTA.

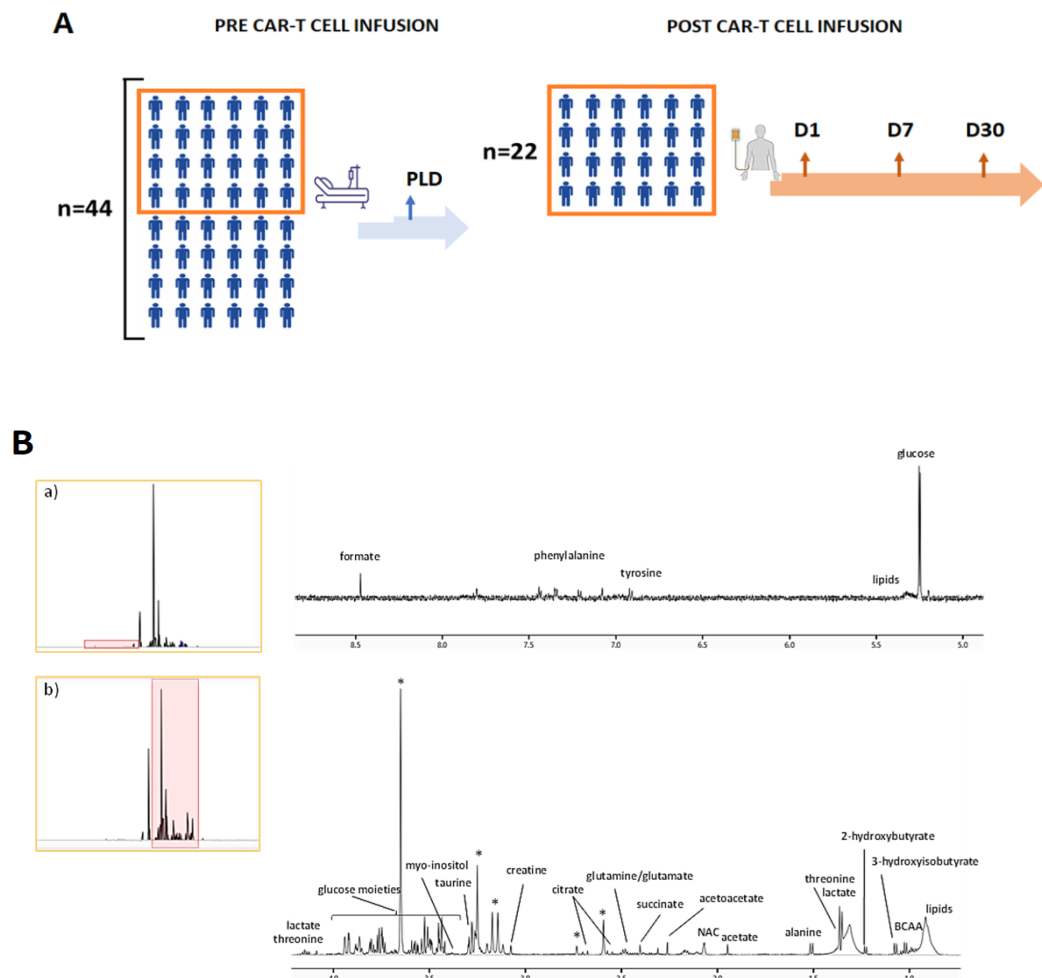


**Figure S2. Principal component analysis (PCA) obtained considering patients at PLD time point.** (A) Scree plot reporting the percentage of variance explained by each component in the model. (B) Principal component 1 and 2 (PC1 vs PC2) loading plot explaining the contribution of the loadings for the first two components. (C) Box-whisker plot distribution of discriminant metabolites between patients stratified according to the last available follow up (CR, n=13, PD, n=26, PR, n=3).

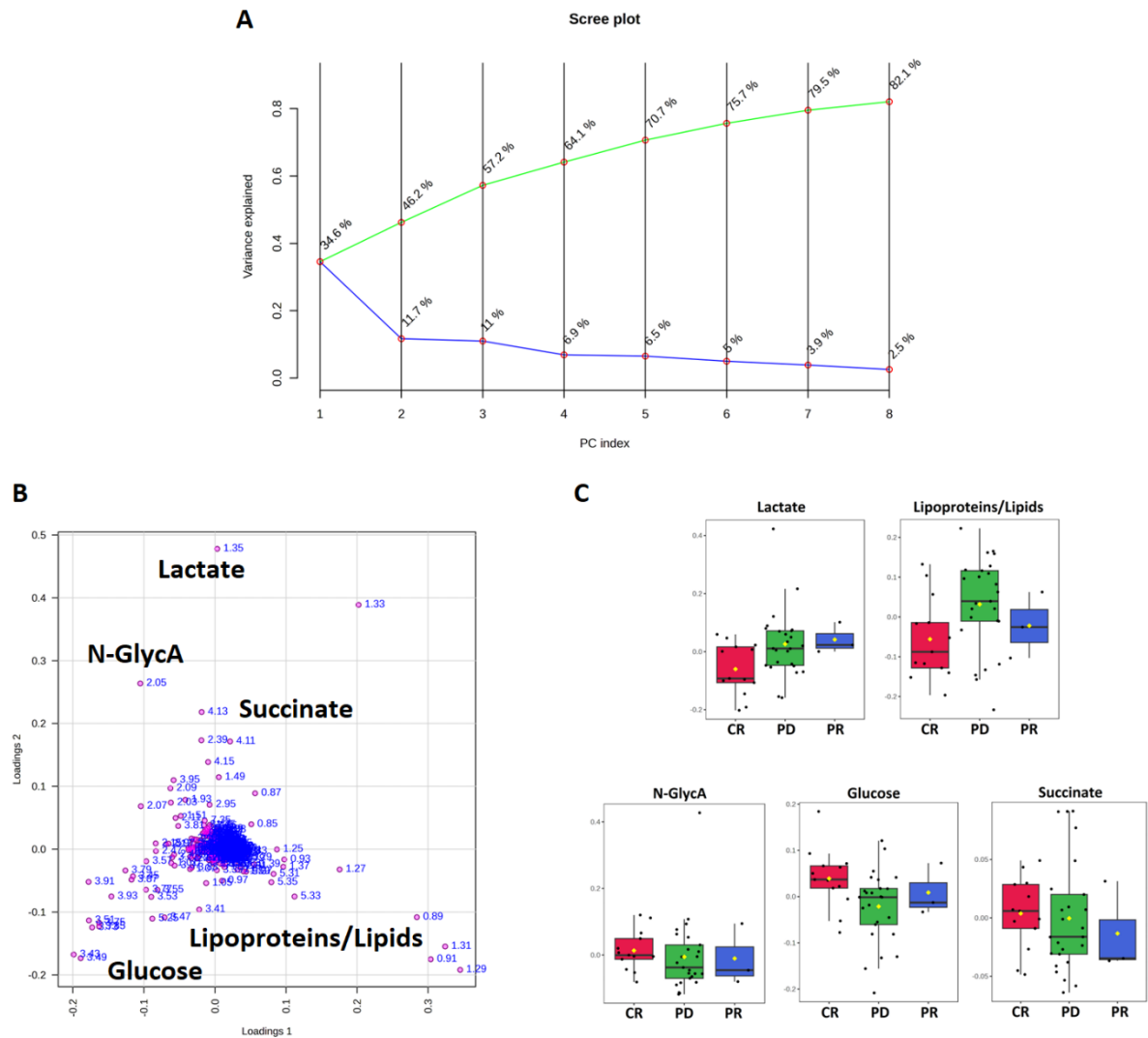


**Figure S3.** Orthogonal partial least squares discriminant analysis (OPLS-DA) for pre-lymphodepletion (PLD) time point in patients treated with axi-cel and tisa-cel.

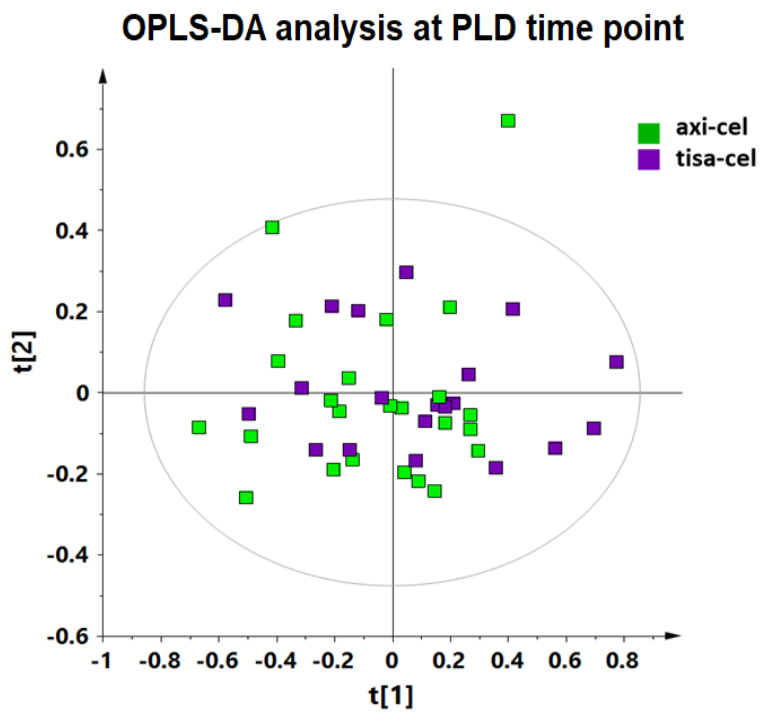


**Figure S4. Circulating plasma profile of N-glycans.** Ten N-glycans were assessed at D30 time point by using "DNA Sequencer Adapted-Fluorophore Assisted Carbohydrate Electrophoresis" (DSA-FACE). The Log of the ratio of the relative abundance of peak 1 (NGA2F) and peak 6 (NA2F) is the GlycoAge Test that is applied between CR patients lasting one year after therapy (CR>D30) (n=12) and those who relapsed within one year (relapsed>D30) (n=8).

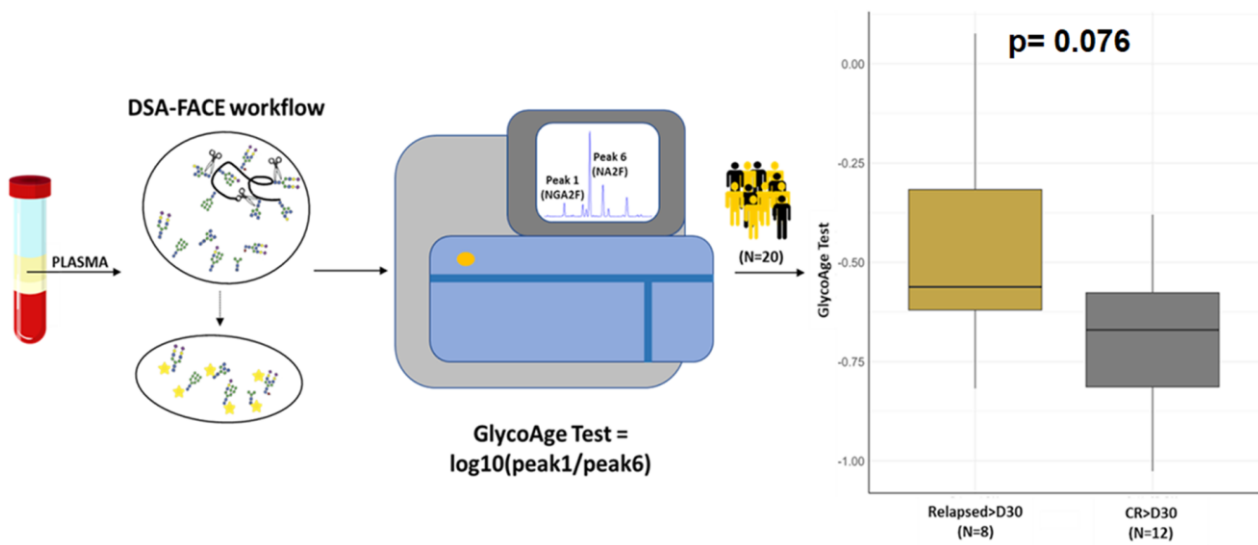




**Table S1.** Chemical shifts ( $\delta$ ) and assignments of metabolites resonances in the  $^1\text{H}$  NMR spectra of the detected human plasma

Metabolites	$^1\text{H}$ NMR chemical shift ( $\delta$ , ppm)
2-hydroxybutyrate	1.13(d); 2.55(m)
3-hydroxybutyrate	1.20(d); 2.31(m)
Acetate	1.92(s)
Acetoacetate	2.22(s)
Alanine	1.48(d); 3.78(q)
Citrate	2.52(d); 2.69(d)
Creatine	3.04(s); 3.93(s)
Formate	8.46(s)
Glutamate	2.10(m); 2.35(m); 3.78(t)
Glutamine	2.14(m); 2.46(m)*; 3.78(t)
Histidine	3.14(m); 3.25(m); 3.99(m); 7.09(s); 7.85(s)
Isoleucine	0.94(t); 1.01(d); 1.26(m); 1.46(m); 1.98(m); 3.67(d)
Lactate	1.33(d); 4.12(q)
Leucine	0.96(d); 0.97(d); 1.70(m); 3.75(m)
Lipoproteins (LDL, VLDL)/lipids	0.87(t); 0.93(m); 1.25(m); 1.29(m); 5.30-5.35(m)
myo-Inositol	3.25(t); 3.61(dd); 4.07(t)
NAC	2.04(s)
Phenylalanine	3.13(m); 3.28(m); 4.00(m); 7.33(d); 7.38(t); 7.43(m)
Pyruvate	2.37 (s)
Succinate	2.41(s)
Tyrosine	3.06(m); 3.20(m); 3.94(m); 6.92(d); 7.20(d)
Taurine	3.25(t); 3.43(t)
Threonine	1.33(d); 3.59(d); 4.25(m)
Tyrosine	3.06(m); 3.20(m); 3.94(m); 6.92(d); 7.20(d)
Valine	0.99(d); 1.04(d); 2.28(m); 3.61(d)
$\alpha$ -Glucose	3.42(t); 3.54(dd); 3.71(t); 3.74(m); 3.84(m); 5.24(d)
$\beta$ -Glucose	3.25(dd); 3.41(t); 3.46(m); 3.49(t); 3.72(dd); 3.90(dd); 4.65(d)

**Table S2.** List of discriminating chemical descriptors (variables) with corresponding correlation coefficient (pcorr), and variable importance on the projection (VIP) for PD vs CR patients OPLS-DA model reported in Figure 2D.

Metabolites (Var ID)	VIP [1+1+0]	p(corr) [1]
Glucose (5.25 ppm)	1.44377	1.06031
Lactate (1.33 ppm)	5.61972	0.598393
Lipoproteins (0.89 ppm)	5.23888	2.38028

**Table S3.** List of discriminating chemical descriptors (variables) with corresponding correlation coefficient (pcorr), and variable importance on the projection (VIP) for tisa-cel vs axi-cel OPLS-DA model reported in Figure 3B.

Metabolites (Var ID)	VIP [1+2+0]	p(corr) [1]
Glucose (5.25 ppm)	1.65228	0.0846376
N-GlycA (2.05 ppm)	3.0474	-0.610006
Acetate (1.93 ppm)	1.08554	0.141068
3-OH butyrate (1.21 ppm)	2.16289	0.359449
Valine (1.01 ppm)	4.95483	-0.170613
Lipoproteins (0.89 ppm)	4.17727	0.351978

**Table S4.** Significance of the Fold change comparison of the discriminant metabolites between CR patients lasting one year after therapy (stable CR>D30) and those who relapsed within one year (relapsed>D30), derived from the unpaired t-test.

Metabolite	Fold Change	Log <sub>2</sub> (FC)	p-value
Histidine	1.5108	0.59535	0.012
N-GlycA	1.507	0.59169	0.024
Phenylalanine	1.3321	0.41372	0.133
Isoleucine	1.3001	0.3786	0.130
Leucine	1.2863	0.36323	0.143
Valine	1.236	0.3057	0.07
Glutamate	1.232	0.30098	0.2165